energies

MDPI

Article

Investigation of PEM Fuel Cell Characteristics in Steady and Dynamic Operation Modes

Alexey Loskutov [1], Andrey Kurkin [2,*], Andrey Shalukho [1], Ivan Lipuzhin [1] and Rustam Bedretdinov [1]

[1] Department of Electric Power Engineering, Power Supply and Power Electronics, Nizhny Novgorod State Technical University n.a. R.E. Alekseev, 603950 Nizhny Novgorod, Russia
[2] Department of Applied Mathematics, Nizhny Novgorod State Technical University n.a. R.E. Alekseev, 603950 Nizhny Novgorod, Russia
* Correspondence: aakurkin@nntu.ru

Abstract: The article is devoted to the problem of proton-exchange membrane fuel cells (PEMFCs) integration into power supply systems. A hybrid energy complex (HEC) based on PEMFCs and lithium iron phosphate batteries can be used as a reliable energy source. It is necessary to properly determine the PEMFC characteristics in order to develop a PEMFC-based HEC prototype and its control algorithms. This paper presents a 1 kW PEMFC's test results in steady and dynamic modes. The dependences of the average hydrogen consumption per 1 min, the volume of hydrogen for the generation of 1 kWh, the PEMFC efficiency on the load current were obtained and an analysis of these dependences for steady operation modes was performed. A range of load changes beyond which the efficiency of the PEMFC significantly decreased and it was recommended to switch to the joint operation of the PEMFCs and batteries (or only batteries) was established. Diagrams of the PEMFC output voltage during the dynamic changes in loads are presented and an analysis of transient response characteristics was carried out. The air supply fans were found to affect the performance of PEMFCs.

Keywords: hydrogen; fuel cell; PEMFC; hybrid energy complex; efficiency; control system

Citation: Loskutov, A.; Kurkin, A.; Shalukho, A.; Lipuzhin, I.; Bedretdinov, R. Investigation of PEM Fuel Cell Characteristics in Steady and Dynamic Operation Modes. *Energies* **2022**, *15*, 6863. https://doi.org/10.3390/en15196863

Academic Editor: Antonino S. Aricò

Received: 27 July 2022
Accepted: 16 September 2022
Published: 20 September 2022

1. Introduction

A key direction in the development of the global electric power industry is associated with the expansion of the use of environmentally friendly low-carbon energy sources. In this regard, more and more attention is paid to fuel cells. Compared to other types of low-carbon sources (wind turbines, photovoltaic modules, etc.), the main advantages of fuel cells are: high efficiency (from 40 to 60%), no noise and vibration during operation and a modular design. This determines the prospects for their wide application in consumer's power supply systems and transport [1,2].

Currently, the most common types of fuel cells are proton-exchange membrane fuel cells (PEMFCs), alkaline electrolyte fuel cells (AFC), phosphoric acid fuel cells (PAFC), molten carbonate fuel cells (MCFC) and solid oxide fuel cells (SOFC) [3]. The choice of fuel cell type depends on the features of its operation, parameters and consumer requirements. PEMFCs are considered the most suitable for power supply of stationary consumers with an installed capacity of up to 50 kW. PEMFC can operate with a high efficiency at low temperatures and are compact in size.

However, the problem of integrating PEMFCs into power supply systems is associated with insufficient maneuverability of the fuel cell. The operation of fuel cells during sudden increases in load is characterized by the fuel starvation problem [4]. The solution is the integrated use of PEMFCs with storage systems based on batteries in a single hybrid energy complex (HEC).

A PEMFC is the main source of energy and ensures the high efficiency of the HEC. The excess power generated by the PEMFC is used to charge the batteries. Batteries provide a

faster response to dynamic load changes compared to PEMFCs [5,6]. Batteries also cover part of the peak load. This allows the use of a fuel cell whose installed power is less than the peak load of the consumer. In addition, the joint use of PEMFCs and batteries allows an increase in the complex autonomy.

Many studies have been devoted to the joint work of PEMFCs and batteries for increasing HEC efficiency. The main areas of research are:

- The improvement of HEC structure;
- The determination of the optimal parameters of the HEC;
- The development of the HEC's control algorithms.

A description of the various structures of an HEC based on fuel cells and batteries is given in [7]. Improving the HEC structure includes modernizing the architecture and increasing the efficiency of input converters [8] and output inverter [9] as part of the HEC. This leads to an increase in power quality, a decrease in power losses and a decrease in the number of components in power converters.

The reliability of the load power supply depends on the correct determination of the HEC parameters. T. Jarry et al. (2021) presented an algorithm for determining the optimal sizing of the hybridized system with a high-temperature PEMFC and battery according to a load profile [7]. J. Rurgladdapan et al. (2013) studied the influence of the number of batteries on the efficiency of the HEC with a fuel cell [10].

The right choice of control strategy allows one to reduce hydrogen consumption while maintaining the battery's state of charge (SOC). Q. Ouyang et al. (2014) developed control algorithms for a hybrid system based on PEMFCs and batteries under dynamic load changes [11]. W.-H. Fang et al. (2014) determined the parameters of the power management system for a stationary hybrid power plant based on simulations in Matlab [12]. M. Cha et al. (2021) presented a power management optimization method for a hybrid electric ferry, where a fuel cell and batteries were used [13].

These studies show that the correct choice of batteries parameters and the adjustment of the HEC control system depends on the accuracy of determining the characteristics of the PEMFC operation in steady and dynamic modes. It is necessary to know how the PEMFC characteristics depend on internal and external factors in various operating modes. The main regularities of PEMFCs' operation have been determined and cannot be disputed. At the same time, the main research method is modeling.

The simulation of fuel cells' operation with a change in hydrogen and oxygen supply is presented in [14,15]. M.S. Pandian et al. (2010) performed an analysis of the dependence between a PEMFC's output power and its efficiency using modeling [16]. K.M. Adegnon et al. (2009) studied the efficiency of PEMFCs based on a simulation in LabView [17]. Most simulation models perform well with slow load changes. However, the qualitative dependence of the PEMFC characteristics on the input parameters obtained by simulation may differ. Thus, M. Sharma et al. (2015) showed that the fuel cell voltage decreased with increasing oxygen pressure and temperature [14]. However, S. Chaudhary et al. (2014) received the opposite nature of these dependencies [18].

R.L. Edwards et al. (2016) presented a simulation model that reflected transient processes during the fuel cell operation with sudden changes in load, as well as a review of research in this area [19].

However, the characteristics of a particular PEMFC (for example, internal resistance) depend on the fuel cell design, manufacturing technology, materials used and material properties changed during operation. Moreover, the ability of a particular PEMFC to respond to dynamic load changes also depends on the degree of the fuel cell degradation and the power consumption of the air supply device (fans or compressor), which is difficult to take into account in simulation.

A. Kulikov et al. (2021) presented a block diagram of a 3 kW HEC based on PEMFCs and batteries for stationary consumers of the railway industry [20]. It used a commercially available 1 kW PEMFC (China) and 3.5 Ah $LiFePO_4$ batteries. The output parameters of the PEMFC and battery were coordinated with each other and with electricity consumers using

a monitoring, protection and control device. The results of the power units' simulation in Simulink were presented. A DC voltage source block with constant internal resistance was used in the model to simulate PEMFCs.

This paper is a continuation of studies presented in [20]. In order to proceed to the stage of development of an HEC prototype, it is mandatory to supplement the results of the simulation, confirming the correctness of the main decisions made, with the results of PEMFC tests and experimental studies that allow one to adjust the parameters of the HEC power unit and more accurately configure the control system. The actual PEMFC operating characteristics, such as hydrogen consumption and efficiency dependencies on hydrogen pressure and load power should be determined for steady operation modes. In addition, it is required to know the ability of PEMFCs to respond to dynamic changes in load. This will accurately determine the parameters of the HEC power unit and more accurately configure the control system.

This article makes a scientific contribution to solving the problem of integration of a PEMFC into power supply systems through a comprehensive analysis of the characteristics of its operation obtained on the basis of experimental studies. On the practical side, these results are intended to adjust the control system of the HEC prototype, which ensures the efficient operation of the HEC in steady-state conditions and a reliable power supply to the load during its dynamic changes.

2. Experimental Methods

2.1. PEMFC Voltage Losses

The voltage U_{PEMFC} is generated at the terminals of the PEMFC electrodes as a result of the ongoing chemical reactions. The dependence of U_{PEMFC} on the load current (I_{PEMFC}) reflects the volt–ampere characteristic (V–I curve) of the fuel cell (Figure 1).

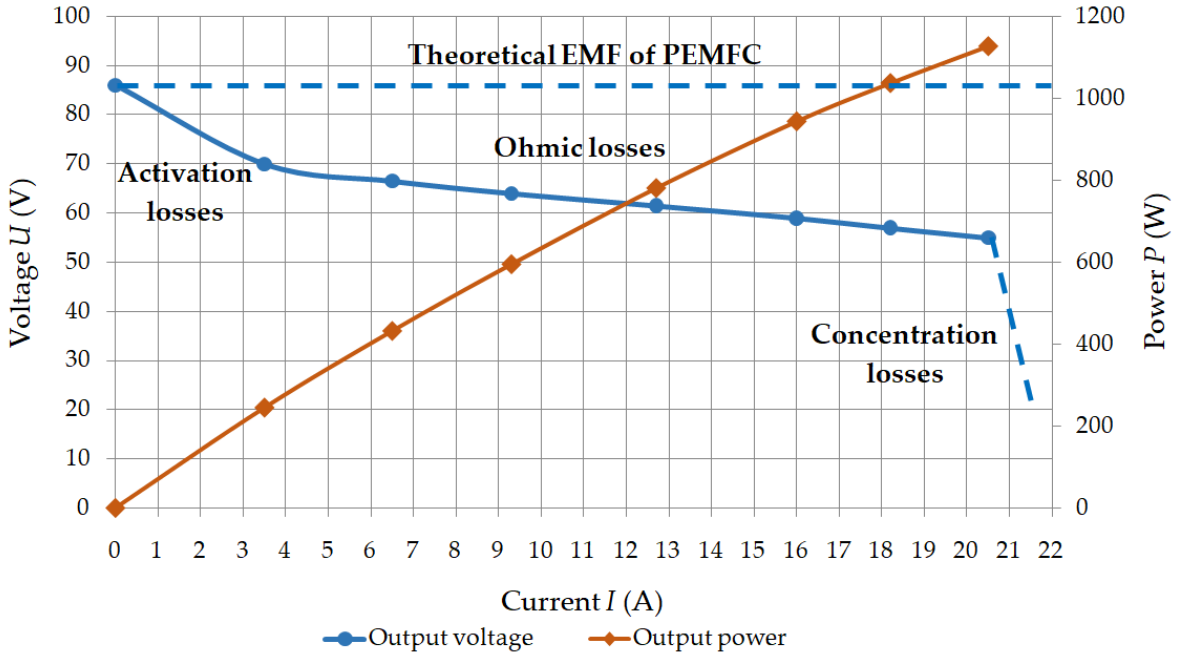

Figure 1. Nominal V–I curve of PEMFC used in HEC.

Three areas of loss in the fuel cell can be distinguished on the V–I curve [4,16,21,22]: activation losses, ohmic losses and concentration losses.

The value of U_{PEMFC} is less than the theoretically possible voltage by the amount of voltage loss in the fuel cell:

$$U_{PEMFC} = E_{theor} - \Delta U_{act} - \Delta U_{ohm} - \Delta U_{conc}, \quad (1)$$

where E_{theor} is the theoretical EMF value of the fuel cell (voltage at the terminals of the fuel cell with an open circuit); ΔU_{act} is the fuel cell activation losses associated with slow reactions on the electrode surfaces; ΔU_{ohm} is the fuel cell ohmic losses associated with voltage drop due to resistive losses in the PEMFC; and ΔU_{conc} is the concentration losses of the fuel cell associated with a decrease in the density of reagents at high currents.

Voltage losses directly affect the efficiency of the PEMFC and HEC as a whole. The higher the value of U_{PEMFC} at the corresponding load current, the lower the voltage loss in the fuel cell and the more efficient the PEMFC operation.

The PEMFC in an HEC is expected to operate in the ohmic loss area most of the time. Ohmic losses are proportional to the resistance of the PEMFC, which includes the resistance to proton current in the membrane and the resistance of the electrodes to the movement of electrons [18]:

$$\Delta U_{ohm} = I_{PEMFC} \times R_{PEMFC} = I_{PEMFC} \times (R_m + R_{el}), \quad (2)$$

where R_{PEMFC} is the PEMFC resistance; R_m is the fuel cell membrane resistance to ion movement; and R_{el} is the resistance of the fuel cell electrodes to the movement of electrons (R_{el} = const).

The HEC power unit's parameters depend on the R_{PEMFC} value [20].

2.2. PEMFC Characteristics in Steady Mode

The following main characteristics are used to assess the PEMFC operation performance in the steady state operation:

- η_{PEMFC} is the PEMFC's electricity generation efficiency (%);
- W_{PEMFC} is the amount of PEMFC-generated electricity (kWh);
- V is the amount of hydrogen used by the PEMFC (L).

The electricity generation efficiency is one of the main characteristics that determine the efficiency of PEMFC operation in steady state. η_{PEMFC} is the ratio of the electricity generated by the fuel cell to the energy that was stored in the hydrogen consumed by this fuel cell:

$$\eta_{PEMFC} = W_{PEMFC}/Q, \quad (3)$$

where Q is the energy stored in the hydrogen supplied to the fuel cell (kJ).

The W_{PEMFC} value can be expressed in kJ (1 kWh = 3.6 kJ):

$$W_{PEMFC} = (U_{PEMFC} \times I_{PEMFC} \times \Delta t \times 3.6)/60; \quad (4)$$

$$P_{PEMFC} = U_{PEMFC} \times I_{PEMFC}, \quad (5)$$

where P_{PEMFC} is the fuel cell output power (kW) and Δt is the time interval at which the electricity generation was determined (min).

The enthalpy of combustion of hydrogen is 286 kJ/mol. The Q value can be determined from measurements of the flow rate of hydrogen, which is converted to the amount of substance, measured in moles:

$$Q = n \times 286, \quad (6)$$

where n is the amount of substance (mol).

The n value can be determined taking into account the PEMFC's operating parameters (hydrogen pressure and temperature) using the ideal gas law:

$$n = (p \times V)/(R \times T), \quad (7)$$

where p is the hydrogen pressure at the PEMFC's inlet (atm); R is the gas constant (R = 0.0821 L·atm/K·mol); and T is the temperature (K).

At the first stage, with the help of experimental studies, the dependence of the η_{PEMFC} and V on the load current (I_{PEMFC}) was obtained for various values of the hydrogen pressure at the PEMFC's inlet (p).

At the second stage, the analysis of the obtained results was carried out and the features of the adjustment of the HEC control system were determined, which ensured the greatest efficiency in steady-state operation.

2.3. PEMFC Characteristics under Dynamic Load Changes

The operation of the PEMFC under dynamic load changes is explained by the typical transient response of a fuel cell (Figure 2a) [19].

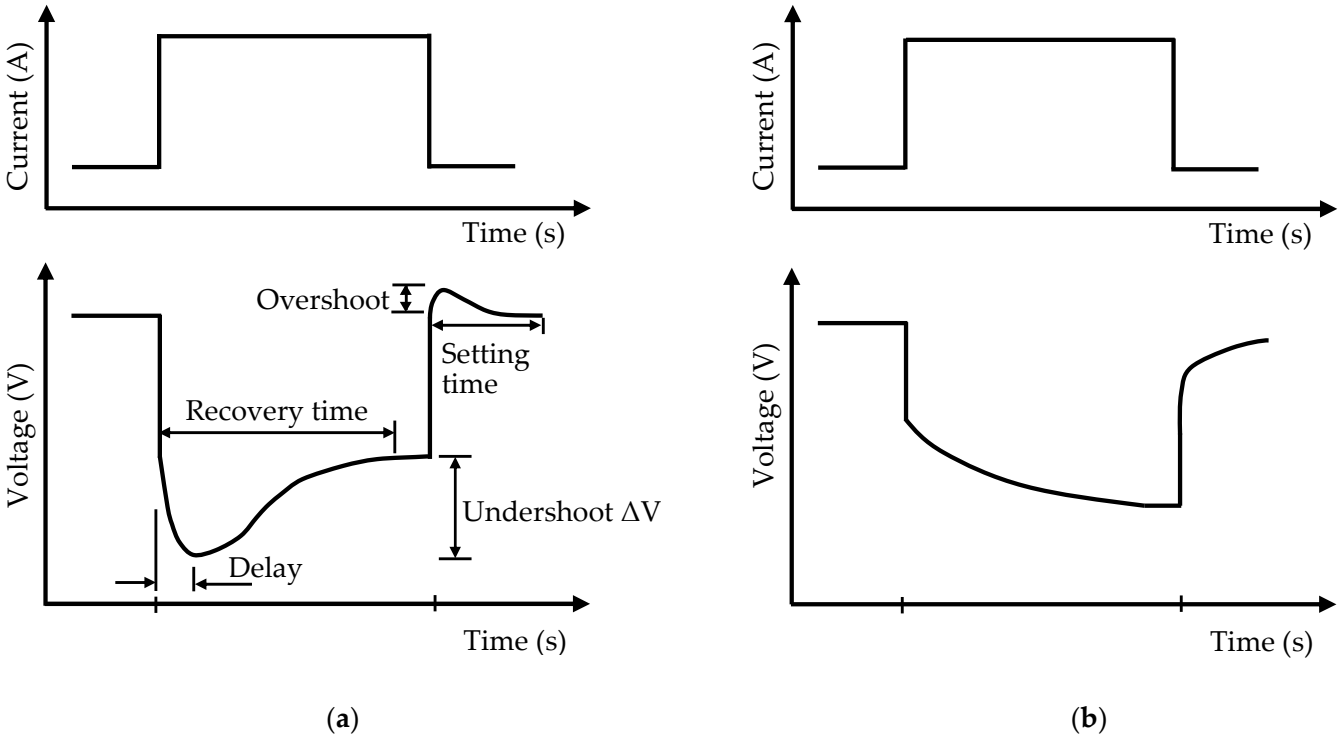

Figure 2. Typical fuel cell (**a**) and batteries' (**b**) transient response.

It can be seen that as the load is increased, the voltage drops to a certain value immediately, but from there, it reaches a new value during the recovery time in an exponential manner [23]. The undershoot behavior is caused by the oxygen starvation. The oxygen concentration reaches the equilibrium condition much slower than hydrogen because of the big difference in gas diffusivity when the load changes. The lower diffusivity of oxygen on the cathode side is the main cause of the significant concentration reduction during load transients [24]. When the current decreases, an overshoot occurs, with subsequent recovery to an equilibrium value [19]. Unlike the case of a step increase in current, only minor oscillations in the cell voltage are observed. The cell performance after a step decrease becomes stable in a shorter period compared to the case of a step increase in current.

Thus, a dynamic change in load is accompanied by a transition process from one stationary state to another. During this process, the PEMFC may suffer from partial overheating or excess air pressure, which will shorten the service life and lead to membrane degradation [25].

Batteries are used as part of the HEC to compensate for dangerous overshoot or undershoot. A typical battery's transient response to a step load current is shown in Figure 2b [26].

The output voltages of batteries, compared to fuel cells in load fluctuation, have faster responses [4]. The combined use of PEMFCs and batteries provide the smoother output characteristics of the HEC. This also improves the performance and extend the service life of the PEMFC [11].

The block diagram and description of the joint use of PEMFCs and batteries were given in [20]. The PEMFC operation under dynamic load changes was investigated to determine the parameters of the HEC power converters, which ensured the joint operation of the PEMFCs and batteries.

The following main characteristics were used to assess PEMFC operation performance under dynamic load changes:

- U_{min} is the minimum voltage value for a dynamic load increase (V);
- U_{max} is the maximum voltage value for a dynamic load decrease (V);
- ΔU_{un} is the voltage undershoot, that is, the difference between U_{min} and the voltage value that is set after a dynamic load increase (V);
- ΔU_{ov} is the voltage overshoot, that is, the difference between U_{max} and the voltage value that is set after a dynamic load decrease (V);
- T_{rec} is the recovery time, that is, the time it takes for the voltage to increase to a steady state value corresponding to the new load current after a dynamic load increase (s);
- T_{set} is the setting time, that is, the time it takes for the voltage to decrease to a steady state value corresponding to the new load current after a dynamic load decrease (s).

At the first stage, the values of the characteristics U_{min}, U_{max}, ΔU_{un}, ΔU_{ov}, T_{rec} and T_{set} were obtained with the help of experimental studies:

- For each initial value of the load current (I_{in}) from 0 to 20 A with a step of 2 A with an increase in load from I_{in} to 22 A in increments of 2 A;
- For each end value of the load current (I_{fin}) from 20 to 0 A with a step of 2 A when the load decreases from 22 A to I_{fin} in steps of 2 A.

As a result, a table with measured data was compiled (Figure 3).

I_{in}	Load increases to current, A										
	2	4	6	8	10	12	14	16	18	20	22
0	…	…	…	…	…	…	…	…	…	…	…
2	x	…	…	…	…	…	…	…	…	…	…
4	x	x	…	…	…	…	…	…	…	…	…
6	x	x	x	…	…	…	…	…	…	…	…
8	x	x	x	x	…	…	…	…	…	…	…
10	x	x	x	x	x	…	…	…	…	…	…
12	x	x	x	x	x	x	…	…	…	…	…
14	x	x	x	x	x	x	x	…	…	…	…
16	x	x	x	x	x	x	x	x	…	…	…
18	x	x	x	x	x	x	x	x	x	…	…
20	x	x	x	x	x	x	x	x	x	x	…

I_{fin}	Load decreases from current, A										
	22	20	18	16	14	12	10	8	6	4	2
20	…	x	x	x	x	x	x	x	x	x	x
18	…	…	x	x	x	x	x	x	x	x	x
16	…	…	…	x	x	x	x	x	x	x	x
14	…	…	…	…	x	x	x	x	x	x	x
12	…	…	…	…	…	x	x	x	x	x	x
10	…	…	…	…	…	…	x	x	x	x	x
8	…	…	…	…	…	…	…	x	x	x	x
6	…	…	…	…	…	…	…	…	x	x	x
4	…	…	…	…	…	…	…	…	…	x	x
2	…	…	…	…	…	…	…	…	…	…	x
0	…	…	…	…	…	…	…	…	…	…	…

Figure 3. General view of table with measured data: … —measurement; x—not defined.

At the second stage, the analysis of the obtained results was carried out and the features of the adjustment of the HEC control system were determined, which ensured a reliable power supply to the consumer during dynamic load changes.

2.4. Test Bench for the Study of PEMFC Operation

Experimental studies of the PEMFC operation were carried out at the NNSTU laboratory using a test bench. The block diagram of the fuel cell test bench is shown in Figure 4.

Hydrogen entered the PEMFC from a gas cylinder (pressure at the outlet of the gas cylinder 150 atm.) through a pressure regulator, which reduced it to a value of 0.6–0.8 atm. The supply of hydrogen was controlled by an inlet solenoid valve. An outlet valve was needed to dump the remaining unused hydrogen. Current and voltage measurements were taken at the PEMFC terminals and separately at the PEMFC air supply fans. The gas flow was measured using a gas flow controller.

The appearance of the fuel cell test bench is shown in Figure 5.

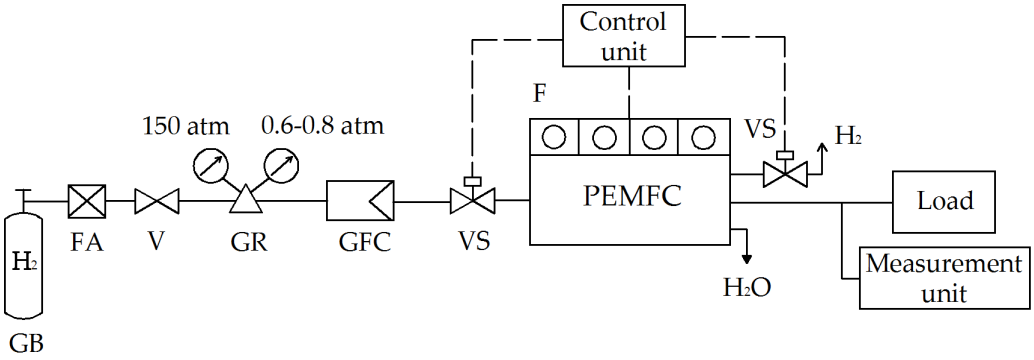

Figure 4. Block diagram of a fuel cell test bench: GB—gas balloon, FA—flashback arrestor; V—valve; GR—gas regulator; GFC—gas flow controller; VS—valve solenoid; F—fan.

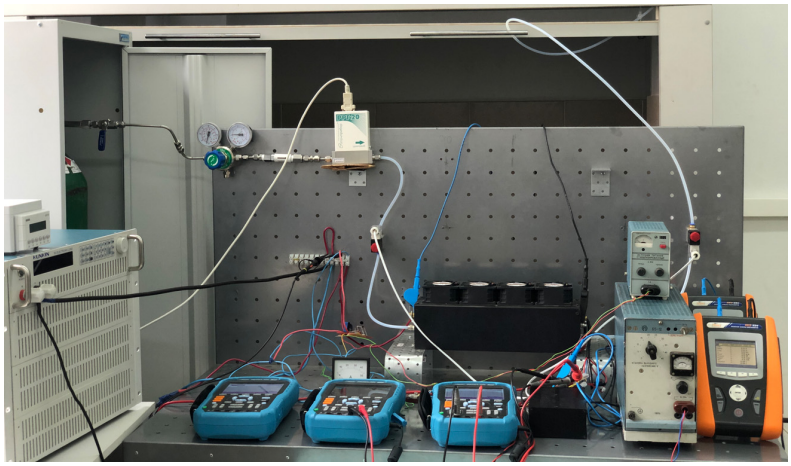

Figure 5. Appearance of the fuel cell test bench.

A commercially available 1000 W PEMFC (Ningbo Vet Energy Technology Co., Ltd.; Ningbo, China) was used. Its main technical data are shown in Table 1.

Table 1. The main technical parameters of the PEMFC.

No.	Parameter	Value, Unit
1	Gas	H_2 (99.99%)
2	PEMFC rated inlet pressure	0.6–0.8 atm
3	PEMFC installed capacity	1 kW
4	PEMFC rated voltage	57 V
5	PEMFC rated current	17.5 A
6	PEMFC air supply fans rated voltage	48 V
7	PEMFC air supply fans quantity and rated power	4 × 62.4 W

The environmental parameters during the experiments were: temperature 24 °C, humidity 50%.

3. Results and Discussion

3.1. Study of PEMFC Voltage Losses and Internal Resistance

The V–I characteristic of the fuel cell depends on the hydrogen pressure at the fuel cell inlet. The PEMFC nominal pressure of hydrogen specified by the manufacturer is 0.6–0.8 atm. The PEMFC operation with other parameters is not recommended. Figure 6 shows the V–I and power characteristics obtained at the boundary values of the nominal hydrogen pressure.

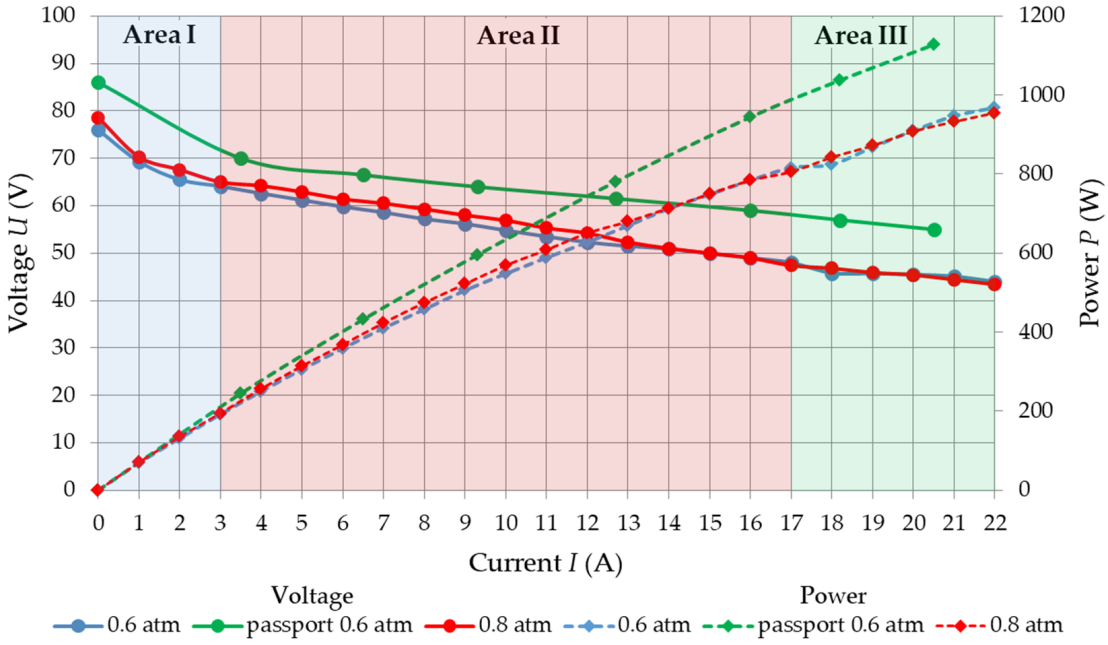

Figure 6. Comparison of the nominal and measured V–I (solid line) and power (dotted) characteristics of PEMFC: green color—nominal at p = 0.6 atm; blue color—measured at p = 0.6 atm; red color—measured at p = 0.8 atm.

The nominal V–I curve in Figure 6 is a manufacturer-declared characteristic of a commercially available PEMFC that was selected for an HEC prototype. The results of the measurements were compared with the nominal V–I curve.

The V–I characteristic of the PEMFC was divided into three areas for further research and analysis of the results:

- Area I is the PEMFC operation at low currents (I_{PEMFC} from 0 to 3 A);
- Area II is the main range of PEMFC operation (I_{PEMFC} from 3 to 17 A);
- Area III is the PEMFC operation at high currents (I_{PEMFC} more than 17 A).

The operation of the PEMFC in the nominal range of hydrogen inlet pressure (0.6–0.8 atm) is characterized by minor changes in the V–I curve. U_{PEMFC} values at p = 0.8 atm slightly exceed the U_{PEMFC} values at p = 0.6 atm. This corresponds to the regularities obtained in [14,15,18].

At the same time, the actual values of U_{PEMFC} in all loss areas are 5–10 V less than the voltages values that correspond to the nominal V–I curve. Therefore, the actual values of U_{PEMFC} in the experimental studies were taken into account when refining the parameters of the HEC power units.

An approximation of the results of the U_{PEMFC} measurements at p = 0.6 atm and 0.8 atm was performed and the equation of a line describing the V–I curve for area II (ohmic losses) was obtained:

$$U_{PEMFC} = 68.011 - 1.211 \times I_{PEMFC}. \quad (8)$$

From Equation (8), it follows that the value of the PEMFC internal resistance R_{PEMFC} = 1.211 Ohm. This value was used to determine the capacitance of the filter compensators in the HEC.

3.2. Studies of PEMFC Characteristics in Steady Mode

The PEMFC hydrogen consumption was measured for 1 min at p = 0.6 atm and 0.8 atm. The RRG-20 regulator (Eltochpribor, LTD; Moscow, Russia) was used for this. Its measuring part is based on the principle of the thermal conversion of gas mass flow into an electrical

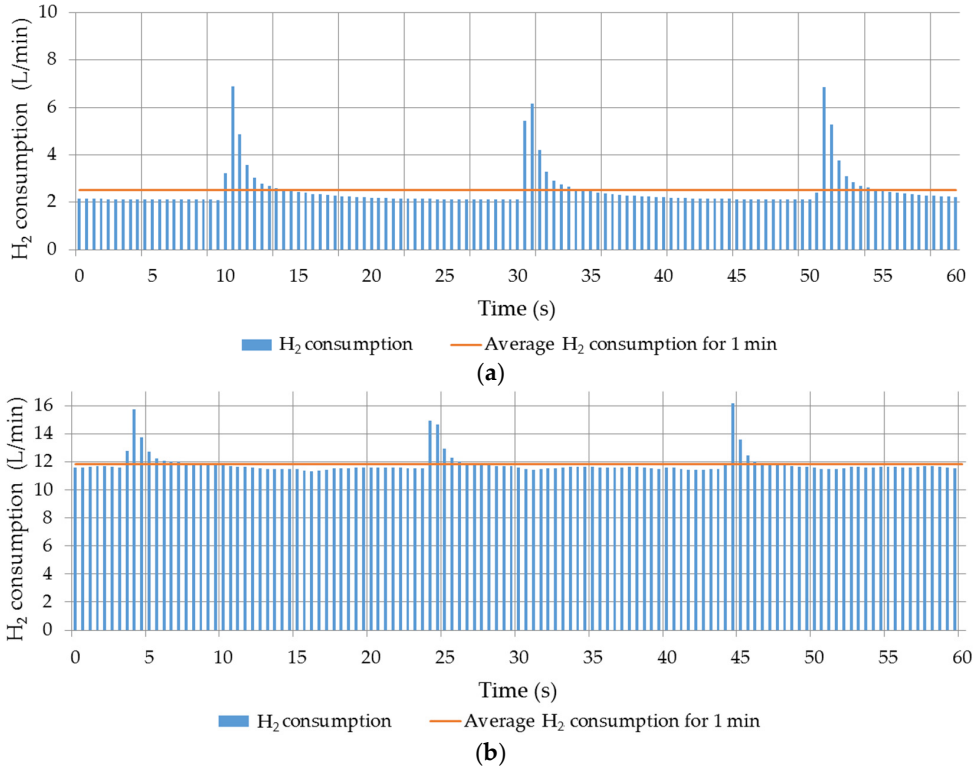

Figure 7. Hydrogen consumption per 1 min at p = 0.6 atm: (**a**) I_{PEMFC} = 1 A; (**b**) I_{PEMFC} = 15 A.

signal. The measurements were carried out when the load changed from 0 to 22 A in steps of 1 A (Figure 7).

Figure 7 shows that the hydrogen consumption is almost constant with periodic peaks that correspond to the opening of the PEMFC outlet valve to purge the anode. The outlet valve is opened at regular intervals. The red line shows the average hydrogen consumption for 1 min. The average hydrogen consumption is proportional to I_{PEMFC}. The larger the I_{PEMFC}, the higher the hydrogen consumption.

The dependence of the average hydrogen consumption per 1 min on the load current at p = 0.6 atm and 0.8 atm is shown in Figure 8.

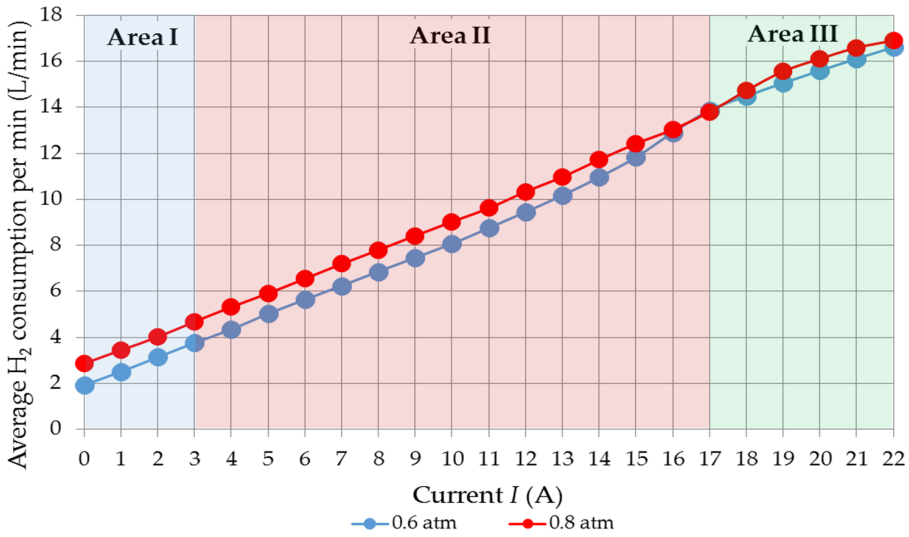

Figure 8. Dependence of the average hydrogen consumption per minute on the load current at p = 0.6 atm (blue line) and 0.8 atm (red line).

From Figure 8, it follows that the dependence of the average hydrogen consumption on the load current is almost linear. The average hydrogen consumption at p = 0.8 atm is approximately 1 L/min higher than at p = 0.6 atm when the PEMFC operates in areas I and II.

The nonload state is present when the load is disconnected (I_{PEMFC} = 0 A). However, there is hydrogen on the anode side, air is supplied on the cathode side (fans running) and the PEMFC is prepared to connect the load. Therefore, the hydrogen consumption is present and minimal even in the nonload state.

The dependencies showing how much hydrogen and time are needed to produce 1 kWh of electricity, depending on the load current and hydrogen pressure at the PEMFC inlet, are shown in Figure 9.

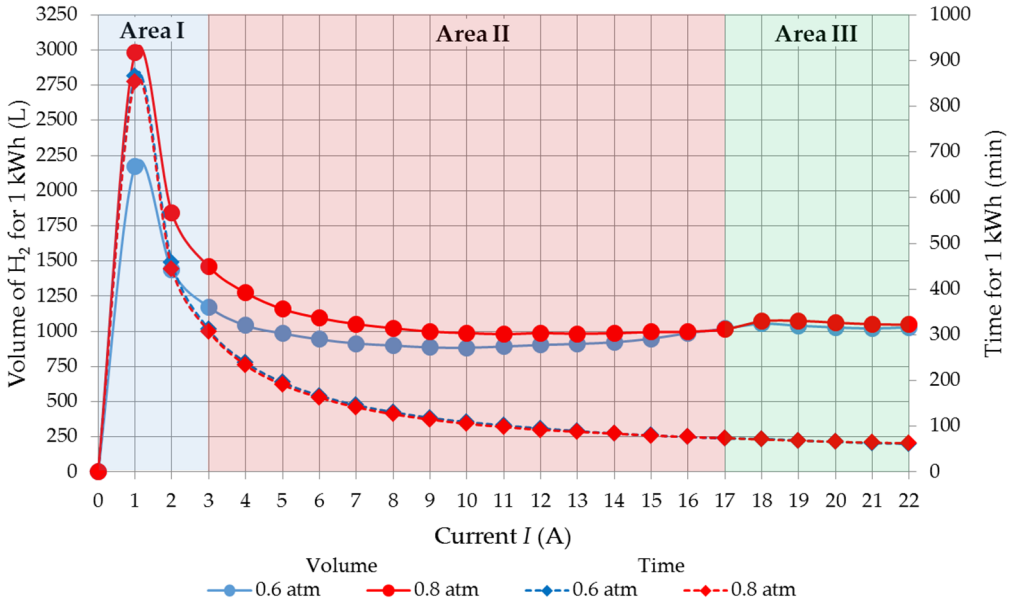

Figure 9. The volume of hydrogen (solid lines) and the time required to generate 1 kWh of electricity (dotted lines) at p = 0.6 atm (blue line) and 0.8 atm (red line).

From Figure 9 it follows that, in general, it takes almost the same time to generate 1 kWh of electricity both at p = 0.6 atm and at 0.8 atm. However, when the PEMFC operates with p = 0.8 atm in areas I and II, a larger volume of hydrogen is required to generate 1 kWh than at p = 0.6 atm. The amount of hydrogen required to generate 1 kWh increases as the load current decreases. Thus, during the PEMFC operation in area I, the hydrogen consumption for generating 1 kWh is more than two times higher than in area II. Therefore, the PEMFC operation in the low load mode (I_{PEMFC} up to 3 A) is not effective. In this case, to increase the HEC efficiency, it seems appropriate to supply the load from the battery.

Based on the measurements of the hydrogen consumption for each point of the V–I curve from 0 to 22 A with a step of 1 A, calculations were performed using Equations (3)–(7) and the values of W_{PEMFC}, Q and η_{PEMFC} were determined. The average temperature T = 25 °C was accepted in the calculations (Figure 10).

The heating of the fuel cell was uneven (Figure 10): in the left part (inlet) the case temperature during the tests reached 42 °C, while in the right part (outlet), the body did not heat up above 30 °C. The maximum temperature during the tests was recorded at the fan blades (due to the air temperature after the cells) at the maximum load (load current 22 A) and amounted to 54 °C. This temperature dropped to 42 °C when the load was dropped.

The dependence of η_{PEMFC} on the load current is shown in Figure 11.

Figure 11 shows that the efficiency is higher when the PEMFC is operated at the lower end of the hydrogen inlet pressure rating range. This can be explained by the fact that, at p = 0.8 atm, the losses of hydrogen increase, which are emitted through the PEMFC outlet

valve. The highest efficiency (about 45%) correspond to the PEMFC operation in area II. In area III, the efficiencies decrease and practically do not change with the increasing current.

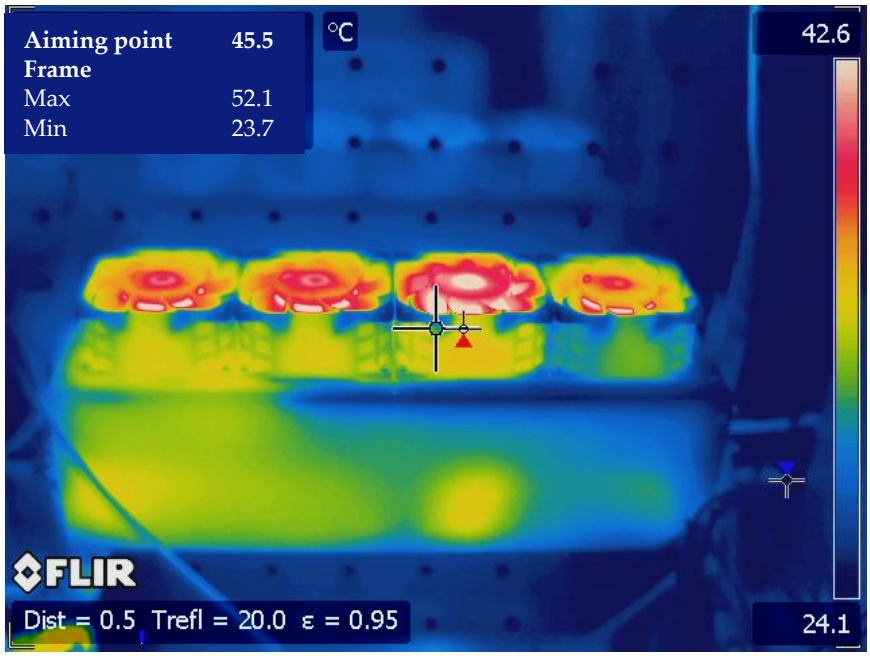

Figure 10. Thermal imaging of PEMFC during testing.

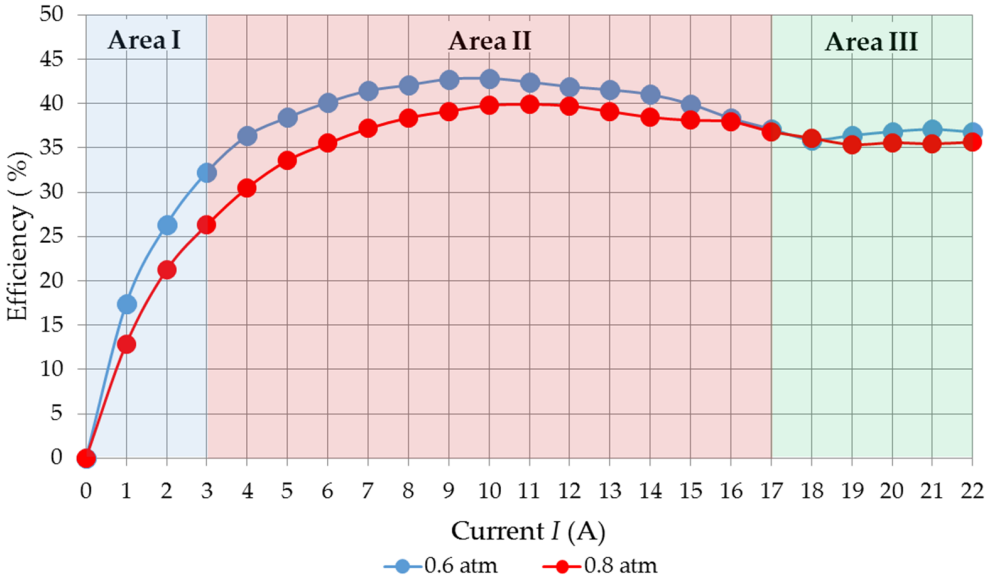

Figure 11. Dependence of η_{PEMFC} on load current at p = 0.6 atm (blue line) and 0.8 atm (red line).

Based on the results of studies on PEMFCs' steady state performance, the following adjustments to the HEC control system are proposed:

1. The voltage values on the V–I curve were closer to the nominal characteristic at p = 0.8 atm (upper limit of the rating range of hydrogen inlet pressure). However, the average hydrogen consumption and the volume of hydrogen required to produce 1 kWh of electricity were lower, and the PEMFC efficiency was correspondingly higher at p = 0.6 atm (the lower limit of the inlet hydrogen pressure rating range). Therefore, it is proposed to maintain a hydrogen inlet pressure of 0.6 atm when the PEMFC operates in steady-state conditions.

2. The highest efficiency of 45% was achieved when the PEMFC operated in area II. In this case, the load (P_{LOAD}) was fully powered by the PEMFC. The excess power generated by PEMFC went to the battery charging (P_{BAT}): $P_{PEMFC} = P_{LOAD} + P_{BAT}$. The PEMFC efficiency dropped to 35% in area III. Therefore, it is proposed to use the PEMFC and battery together at load currents of more than 17 A. In this case, part of the load receives power from the batteries. This will reduce the required power from the PEMFC and move the PEMFC operation to area II: $P_{PEMFC} = P_{LOAD} - P_{BAT.}$ Thus, the PEMFC will be most efficient when operating as part of the HEC.
3. It was established that the efficiency was about 25%, and the amount of hydrogen required to produce 1 kWh of electricity was almost two times higher when the PEMFC operated in area I than in area II. Therefore, it is proposed to switch to powering the load only from the battery (provided that the battery charge is sufficient) to increase the HEC autonomy at low loads (up to 3 A).

Thus, region II (ohmic loss region) is the most effective for the PEMFC operation in steady-state conditions.

The main provisions of the power distribution strategy between the PEMFC and batteries were determined based on the research results (Table 2).

Table 2. Power distribution strategy between the fuel cell and the battery in HEC.

Load Mode (I_{LOAD}, A)	Cases (Battery SOC)	Load Power P_{LOAD}	Control Strategy
<3	SOC_{min}	$P_{PEMFC} - P_{BAT}$	PEMFC powers the load and charges the batteries. I_{PEMFC} maintained between 3 and 17 A.
	$SOC_{min} \ldots SOC_{max}$	P_{BAT}	The load is powered by batteries.
	SOC_{max}		The control system monitors the battery's charge.
3 … 17	SOC_{min}	$P_{PEMFC} - P_{BAT}$	Efficient operating mode. Surplus generation goes to charge the battery. Battery's charge is controlled to keep I_{PEMFC} between 3 and 17 A
	$SOC_{min} \ldots SOC_{max}$		
	SOC_{max}	$P_{PEMFC} + P_{BAT}$	
>17	SOC_{min}	$P_{PEMFC} - P_{BAT}$	Undesirable operating mode. The power is shared between PEMFC and battery in such a way as to keep I_{PEMFC} between 3 and 17 A
	$SOC_{min} \ldots SOC_{max}$		
	SOC_{max}	$P_{PEMFC} + P_{BAT}$	

Note: I_{LOAD} is a load current at a given time; I_{PEMFC} is a PEMFC current; SOC_{min} and SOC_{max} are the minimum allowable and maximum possible battery SOC level.

A more detailed study of the power distribution between the fuel cell and battery is an important task for future work.

3.3. Studies of PEMFC Characteristics under Dynamic Load Changes

A series of experiments was carried out, in which the load current instantly increased from an initial value (I_{in}) to a predetermined end value (I_{fin}) and, after reaching the steady state, again instantly decreased to I_{in}.

The obtained diagrams of U_{PEMFC} changes for various values of I_{in} are shown in Figure 12.

From Figure 12, it follows that the diagrams of U_{PEMFC} changes, depending on the features of their characteristics, can be divided into three groups:

- Group 1—a change of U_{PEMFC} with a dynamic change of load current at I_{in} from 0 to 8 A. The U_{PEMFC} curves are fully consistent with a typical fuel cell's transient response (Figure 3). It is possible to determine U_{min}, U_{max}, ΔU_{un} and ΔU_{ov} based on these diagrams and plot their dependencies.
- Group 2—a change of U_{PEMFC} with a dynamic change of load current at I_{in} from 10 to 18 A. The U_{PEMFC} curves differ from the typical fuel cell's transient response. U_{PEMFC} fluctuations are observed during the dynamic load changes, which are characterized

by a high frequency at small amplitudes (several volts). It is not possible to accurately determine the characteristics ΔU_{un}, ΔU_{ov}, T_{rec} and T_{set}.

- Group 3—a change of U_{PEMFC} with a dynamic change of load current at I_{in} from 20 to 22 A. The U_{PEMFC} curves are characterized by the fact that the fluctuations become much smaller, and the pattern correlates with the typical fuel cell transient response.

The U_{PEMFC} fluctuations in the diagrams from group 2 can be explained by the operation of the fans, which provide air supply. Figure 13 shows a diagram of the change in the power consumption of the fans depending on the load current.

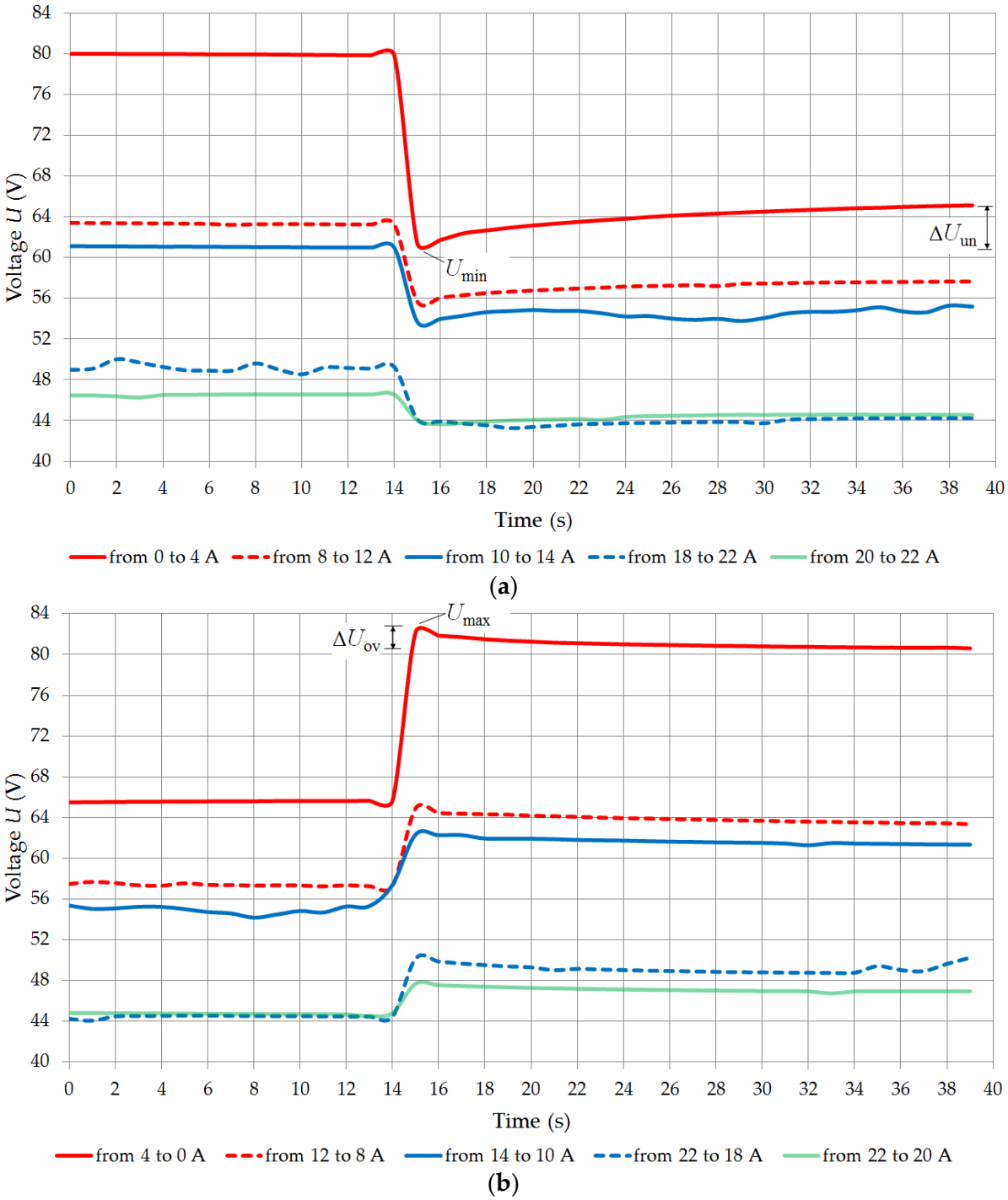

Figure 12. Diagrams of changes in PEMFC output voltage U_{PEMFC} with a change in the load current: (**a**) load increase; (**b**) load decrease.

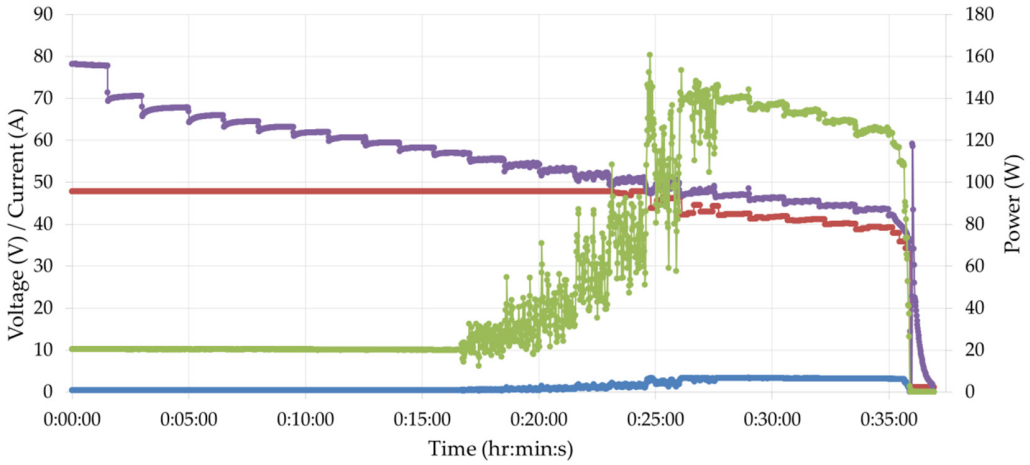

Figure 13. Characteristics of air supply fans: current (blue line), voltage (red) and power (green) of fans and voltage at the PEMFC output (purple line) during tests.

A DC/DC step-down converter provides a 48 V rated voltage to the air supply fans. The DC/DC converter is powered directly from the PEMFC output. At I_{in} from 0 to 10 A, the fans constantly consume the same power, equal to 20 W. The PEMFC output voltage curves correspond to those of a typical fuel cell's transient response (no voltage fluctuations) over this interval. In the interval I_{in} from 10 to 18 A, the power consumed by the fans increases from 20 to 160 W. At the same time, significant fluctuations in power consumption (with an amplitude of up to 40 W) are observed over the entire interval. This can be explained by the incorrect choice of settings in the voltage feedback circuit, which is used in the PEMFC control system. This leads to fluctuations in the supply of air necessary for the operation of the fuel cell, which, with dynamic changes in the load, leads to fluctuations in U_{PEMFC}. The power consumed by the fans stabilizes again (at approximately 130 W) when I_{in} reaches 20 A. As a result, the U_{PEMFC} fluctuations disappear at I_{in} = 20 A. It should also be taken into account that when the voltage at the PEMFC output drops below 48 V, the fans stop receiving the required voltage of 48 V, which begins to gradually decrease, reaching 40 V at the rated load of the PEMFC. It also influences the fluctuation of the power consumption of the fans.

It is proposed to add an additional separate source in the HEC structure to power the air supply fans in order to stabilize the operation of the PEMFC during dynamic load changes. The power consumed by the fans will be set depending on the load current.

The values U_{min}, U_{max}, ΔU_{un} and ΔU_{ov} were determined for the U_{PEMFC} change diagrams belonging to groups 1 and 3. Based on the diagrams from group 2, it was only possible to determine the values U_{min} and U_{max}.

Figure 14 shows the dependencies of the values U_{min} on I_{fin} and U_{max} on I_{in}.

The lower the PEMFC output voltage dropped, the greater the end load current (I_{fin}) was during a dynamic load increase. The voltage dropped lower at smaller values of I_{in} for the same I_{fin}. U_{PEMFC} decreased to 35 V and PEMFC turned off when the load increased from 0 to 22 A (I_{in} = 0 A; I_{fin} = 22 A). The obtained results confirmed that dynamic load increases to maximum values when PEMFC is operating in a mode close to idle were the most dangerous.

In general, with a dynamic decrease in load, similar dependences of PEMFC characteristics were observed as with an increase in load. The PEMFC output voltage increased as the difference between I_{fin} and I_{in} increased. The highest output voltage values were observed when the load decreased from 22 to 0 A.

Figure 15 shows the dependencies of the values ΔU_{un} on I_{fin} and ΔU_{ov} on I_{in}.

The ΔU_{UN} values characterize the recovery of the PEMFC output voltage after a transient. The greater the values of ΔU_{un} are, the lower the value of the initial load current I_{in} for the same I_{fin}.

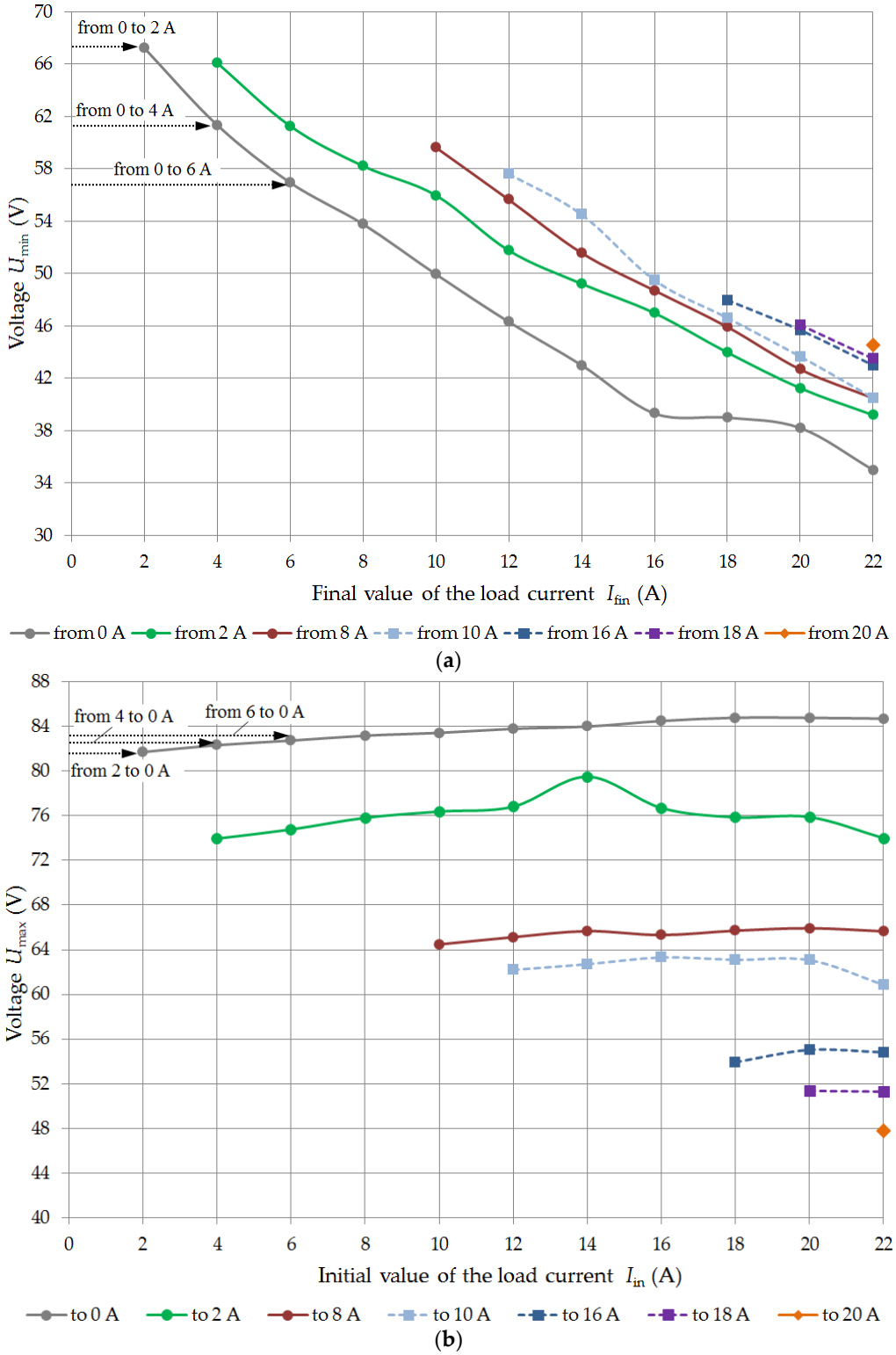

Figure 14. Dependencies of PEMFC characteristics under dynamic load increase: (**a**) U_{min} on I_{fin}; (**b**) U_{max} on I_{in}.

The results of our studies showed that the power supply of consumers could be disrupted with sudden changes in load if only the PEMFC was used. Therefore, it is necessary to use batteries together with the PEMFC to provide power to the load when it changes abruptly. After the PEMFC catches up with the power demand, the battery,

depending on the level of its charge, will continue to be partially discharged (at a large SOC) or will be charged from the PEMFC (at a low SOC).

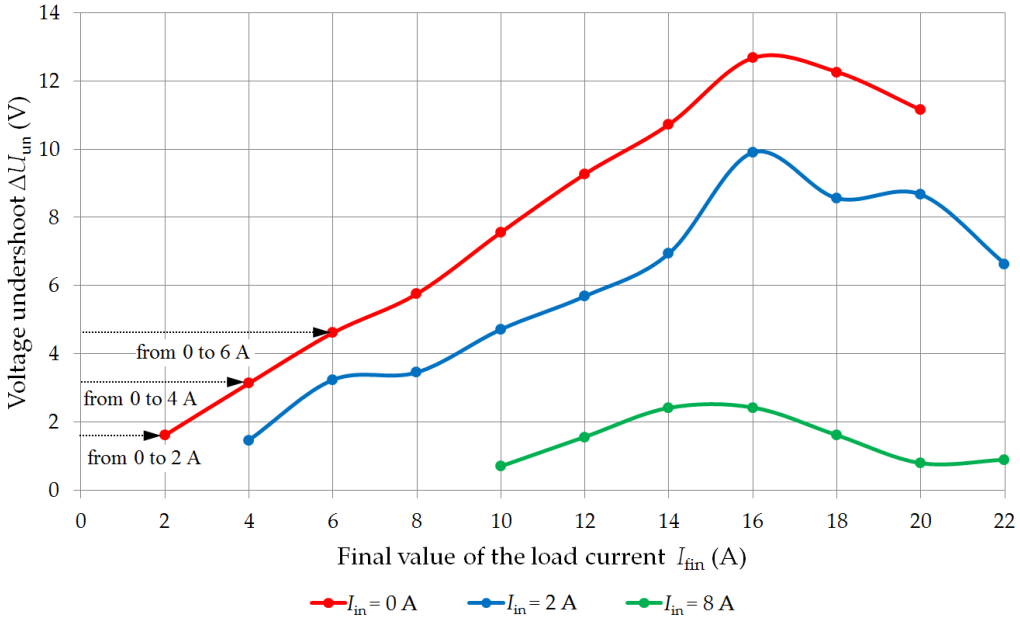

(**a**)

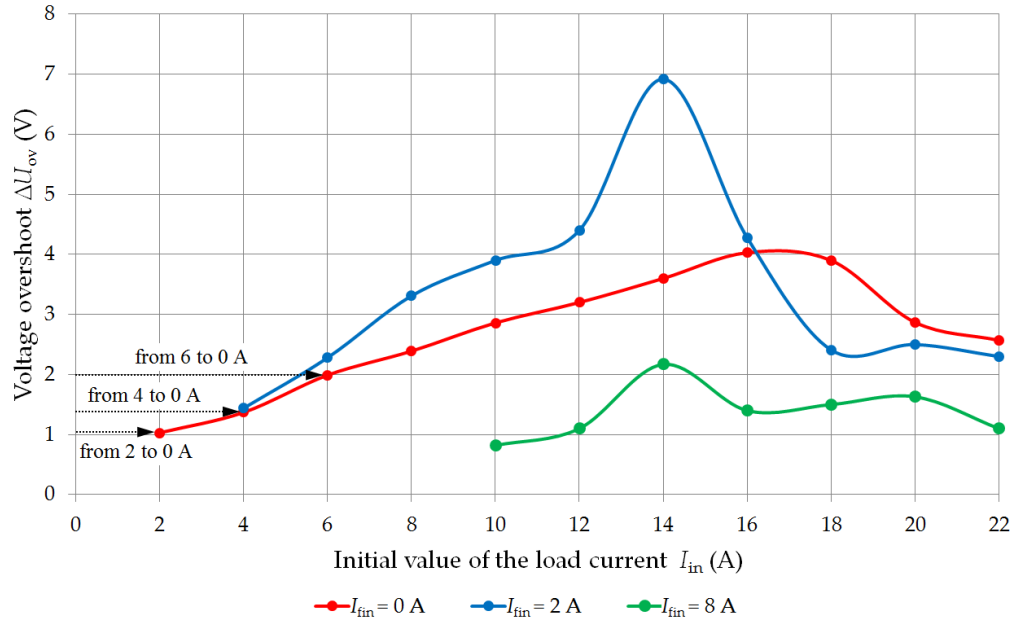

(**b**)

Figure 15. Dependencies of PEMFC characteristics under dynamic load decrease: (**a**) ΔU_{un} on I_{fin}; (**b**) ΔU_{ov} on I_{in}.

The results of the experimental studies of the PEMFC characteristics under dynamic load changes can be used to determine the battery capacity. Moreover, the dependences of U_{min} and ΔU_{un}, as well as U_{max} and ΔU_{ov} can be used to determine the parameters of the HEC's input converter. The input voltage range of the converter must ensure the operation of the PEMFC when its voltage changes from the lowest value U_{min} to the highest value U_{max}.

4. Conclusions

PEMFCs are considered the most efficient type of fuel cells for power supply of stationary consumers up to 50 kW. However, PEMFCs are characterized by an insufficient maneuverability under dynamically changing loads. This problem was solved by combining PEMFCs with batteries in a single hybrid energy complex (HEC).

A prototype of an HEC based on PEMFCs and lithium-iron-phosphate batteries for supplying stationary consumers of the railway industry is being developed at NNSTU. Experimental studies of the PEMFC operation in steady and dynamic modes were carried out to proceed to the stage of creating the HEC prototype.

The value of the PEMFC internal resistance (R_{PEMFC} = 1.211) was determined based on the approximation of the measurement results for the area of ohmic losses. It will be used to determine the capacitance of the filter compensators in the HEC.

It was established that the highest efficiency (about 45%) was achieved when the PEMFC operated in the area of ohmic losses. The results of our experimental studies of the PEMFC performance under steady modes will be used to adjust the HEC control system:

- The PEMFC continuous operation in the area of activation losses was characterized by an overestimated consumption of hydrogen for electricity generation and a low efficiency (no more than 25%); therefore, it is proposed to switch the power supply of consumers to batteries at low loads;
- The PEMFC operation in the area of concentration losses was characterized by an efficiency of about 35%; therefore, it is proposed to use the PEMFC and AB jointly to increase the efficiency of the PEMFC and HEC as a whole at high load currents.

Studies were carried out on the characteristics of the PEMFC under dynamic load changes. The air supply fans affected the performance of the PEMFC. Significant fluctuations in the PEMFC output voltage were observed with load dynamic changes when the PEMFC was operated in the load range from 10 to 18 A. An additional separate power supply for air supply fans is proposed to be added to the HEC structure to stabilize the PEMFC operation during dynamic load changes. The analysis of the dependences of the characteristics U_{min}, U_{max}, ΔU_{un} and ΔU_{ov} on the initial and end load currents will be used to determine the parameters of the HEC input converter.

Future work will include:

- The development of an HEC prototype taking into account the results of the study of the PEMFC characteristics;
- The development of HEC control system software;
- Studies of the HEC and the joint operation of the PEMFC and battery in real operation conditions.

Author Contributions: Conceptualization, A.L. and A.K.; methodology, A.L., A.K. and A.S.; validation, I.L.; formal analysis, A.S.; investigation, I.L. and R.B.; writing—original draft preparation, A.L., A.K., A.S. and I.L.; writing—review and editing, A.L. and A.K.; visualization, R.B.; supervision, A.L. and A.K.; project administration, A.L. and A.K. All authors have read and agreed to the published version of the manuscript.

Funding: The reported study was funded by RFBR, Sirius University of Science and Technology, JSC Russian Railways and Educational Fund "Talent and success", project number 20-38-51016 and Council of the grants of President of the Russian Federation for the state support of Leading Scientific Schools of the Russian Federation (grant no. NSH-70.2022.1.5).

Conflicts of Interest: The authors declare no conflict of interest.

References

1. Zhou, D.; Ravey, A.; Al-Durra, A.; Gao, F. A comparative study of extremum seeking methods applied to online energy management strategy of fuel cell hybrid electric vehicles. *Energy Convers. Manag.* **2017**, *151*, 778–790. [CrossRef]
2. Meng, X.; Li, Q.; Zhang, G.; Wang, T.; Chen, W.; Cao, T. A dual-mode energy management strategy considering fuel cell degradation for energy consumption and fuel cell efficiency comprehensive optimization of hybrid vehicle. *IEEE Access* **2019**, *7*, 134475–134487. [CrossRef]
3. Godula-Jopek, A.; Westenberger, A.F. Fuel Cell Types: PEMFC/DMFC/AFC/PAFC//MCFC/SOFC/. In *Encyclopedia of Energy Storage*; Cabeza, L.F., Ed.; Elsevier: Amsterdam, The Netherlands, 2022; Volume 2, pp. 250–265. [CrossRef]
4. Hsu, S.; Liang, S. Optimal efficiency of fuel cell/battery hybrid power management. In Proceedings of the 2012 International Conference on Control, Automation and Information Sciences (ICCAIS), Saigon, Vietnam, 26–29 November 2012; pp. 231–235. [CrossRef]
5. Xie, C.; Xu, X.; Bujlo, P.; Shen, D.; Zhao, H.; Quan, S. Fuel cell and lithium iron phosphate battery hybrid powertrain with an ultracapacitor bank using direct parallel structure. *J. Power Sources* **2015**, *279*, 487–494. [CrossRef]
6. Yu, Y.; Li, Q.; Chen, W.; Su, B.; Liu, J.; Ma, L. Optimal energy management and control in multimode equivalent energy consumption of fuel cell/supercapacitor of hybrid electric tram. *IEEE Trans. Ind. Electron.* **2019**, *66*, 6065–6076. [CrossRef]
7. Jarry, T.; Lacressonnière, F.; Jaafar, A.; Turpin, C.; Scohy, M. Optimal sizing of a passive hybridization fuel cell–battery. In Proceedings of the 2021 International Conference on Electrical, Computer and Energy Technologies (ICECET), Cape Town, South Africa, 9–10 December 2021; pp. 1–6. [CrossRef]
8. Wang, B.; Xian, L.; Manandhar, U.; Ye, J.; Ukil, A.; Beng Gooi, H. A stand-alone hybrid PV/fuel cell power system using single-inductor dual-input single-output boost converter with model predictive control. In Proceedings of the 2017 Asian Conference on Energy, Power and Transportation Electrification (ACEPT), Singapore, 24–26 October 2017; pp. 1–5. [CrossRef]
9. Yadav, S.S.; Sandhu, K.S. A Five –level PWM Inverter for hybrid PV/fuel cell/battery standalone power system. In Proceedings of the 2018 IEEE International Students' Conference on Electrical, Electronics and Computer Science (SCEECS), Bhopal, India, 24–25 February 2018; pp. 1–6. [CrossRef]
10. Rurgladdapan, J.; Uthaichana, K.; Kaewkhamai, B. Optimal Li-Ion battery sizing on PEMFC hybrid powertrain using dynamic programming. In Proceedings of the 2013 IEEE 8th Conference on Industrial Electronics and Applications (ICIEA), Melbourne, VIC, Australia, 19–21 June 2013; pp. 472–477. [CrossRef]
11. Ouyang, Q.; Wang, F.; Chen, J.; Li, X. Power management of PEM fuel cell hybrid systems. In Proceedings of the 33rd Chinese Control Conference, Nanjing, China, 28–30 July 2014; pp. 7082–7087. [CrossRef]
12. Fang, W.-H.; Guo, Y.-F.; Wang, F.-C. The development and power management of a stationary PEMFC hybrid power system. In Proceedings of the 2015 IEEE/SICE International Symposium on System Integration (SII), Nagoya, Japan, 11–13 December 2015; pp. 684–689. [CrossRef]
13. Cha, M.; Jayasinghe, S.G.; Enshaei, H.; Islam, R.; Abeysiriwardhane, A.; Alahakoon, S. Power management ptimization of a battery/fuel cell hybrid electric ferry. In Proceedings of the 2021 31st Australasian Universities Power Engineering Conference (AUPEC), Perth, Australia, 26–30 September 2021; pp. 1–6. [CrossRef]
14. Sharma, M.; Pachauri, R.K.; Goel, S.K. MATLAB/Simulink modeling and analysis of parametric effects on PEMFC performance. In Proceedings of the 2015 International Conference on Recent Developments in Control, Automation and Power Engineering (RDCAPE), Noida, India, 12–13 March 2015; pp. 226–231. [CrossRef]
15. Belmokhtar, K.; Hammoudi, M.; Doumbia, M.L.; Agbossou, K. Modelling and fuel flow dynamic control of proton exchange membrane fuel cell. In Proceedings of the 4th International Conference on Power Engineering, Energy and Electrical Drives, Istanbul, Turkey, 13–17 May 2013; pp. 415–420. [CrossRef]
16. Pandian, M.S.; Anwari, M.; Husodo, B.Y.; Hiendro, A. Efficiency and economics analysis of proton exchange membrane fuel cell. In Proceedings of the 2010 International Power Engineering Conference (IPEC), Singapore, 27–29 October 2010; pp. 875–880. [CrossRef]
17. Adegnon, K.M.; Dube, Y.; Agbossou, K. Experimental evaluation of PEM fuel cell systems efficiency. In Proceedings of the 2009 Canadian Conference on Electrical and Computer Engineering, St. John's, NL, Canada, 3–6 May 2009; pp. 716–719. [CrossRef]
18. Chaudhary, S.; Chauhan, Y.K. Studies and performance investigations on fuel cells. In Proceedings of the 2014 International Conference on Advances in Engineering and Technology Research (ICAETR 2014), Unnao, India, 1–2 August 2014; pp. 1–6. [CrossRef]
19. Edwards, R.L.; Demuren, A.O. Regression analysis of PEM fuel cell transient response. *Int. J. Energy Environ. Eng.* **2016**, *7*, 329–341. [CrossRef]
20. Kulikov, A.; Loskutov, A.; Kurkin, A.; Dar'enkov, A.; Kozelkov, A.; Vanyaev, V.; Shahov, A.; Shalukho, A.; Bedretdinov, R.; Lipuzhin, I.; et al. Development and operation modes of hydrogen fuel cell generation system for remote consumers' power supply. *Sustainability* **2021**, *13*, 9355. [CrossRef]
21. Guaitolini, S.V.M.; Yahyaoui, I.; Fardin, J.F.; Encarnação, L.F.; Tadeo, F. A review of fuel cell and energy cogeneration technologies. In Proceedings of the 2018 9th International Renewable Energy Congress (IREC), Hammamet, Tunisia, 20–22 March 2018; pp. 1–6. [CrossRef]
22. Barbir, F.; Gomez, T. Efficiency and economics of proton exchange membrane (PEM) fuel cell. *Int. J. Hydrogen Energy* **1997**, *22*, 1027–1037. [CrossRef]

23. Seyezhai, R.; Mathur, B.L. Mathematical modeling of proton exchange membrane fuel cell. *Int. J. Comput. Appl.* **2011**, *20*, 1–6.
24. Kim, H.; Min, K. Experimental investigation of dynamic responses of a transparent PEM fuel cell to step changes in cell current density with operating temperature. *J. Mech. Sci. Technol.* **2008**, *22*, 2274–2285. [CrossRef]
25. Zhu, X.; Xu, D.; Chen, P. Energy management analysis and design for a 5 kW PEMFC distributed power system. In Proceedings of the 2008 IEEE Power Electronics Specialists Conference, Rhodes, Greece, 15–19 June 2008; pp. 2288–2294. [CrossRef]
26. Chen, M.; Rincon-Mora, G.A. Accurate electrical battery model capable of predicting runtime and I–V performance. *IEEE Trans. Energy Convers.* **2006**, *21*, 504–511. [CrossRef]